Transcription factor FOXM1 specifies the loading of chromatin DNA to extracellular vesicles

Yunsheng Zhang[1,2], Nana Ding[1], Yizhen Li[1], Xiaoyun Zhao[1], Shiping Yang[1], Ping Fu[1], Yousong Peng[1], Haojie Cheng[1], Min Ouyang[1], Ruiping Wang[1], Yu Wang[1], Hanyun Liu[1], Yan Chen[1], Xiaoqin Huang[1], Li Yu[1], and Yongjun Tan[1*]

[1] State Key Laboratory of Chemo/Biosensing and Chemometrics, College of Biology, Hunan Engineering Research Center for Anticancer Targeted Protein Pharmaceuticals, Hunan University, Changsha, Hunan 410082, PR China.

[2] The Second Affiliated Hospital, University of South China, Hengyang, Hunan 421001, PR China.

**** Correspondence to:*** Dr. Yongjun Tan, E-mail: yjtan@hnu.edu.cn

Abstract

Extracellular vesicle DNAs (evDNAs) possess the important diagnostic value for multiple diseases and play roles for horizontally transferring genetic materials among cells. In this study, we have found that transcription factor FOXM1 can mediate the loading of certain chromatin genes or DNA fragments (named FOXM1-chDNAs) to extracellular vesicles (EVs). FOXM1 interacts with LC3 in nucleus and FOXM1-chDNAs (such as *DUX4* gene and Telomere DNA) are specified by FOXM1 and translocated to cytoplasm. These DNAs are released to EVs through the process of an LC3-involved autophagosome-multivesicular body (MVB) transport. The roles of FOXM1 on loading FOXM1-chDNAs to EVs are further confirmed by DNA-FISH experiments, tracing the translocation of selected chromatin loci with the TetO/TetR-GFP method, and PCR analysis of the DNA samples from MVBs and EVs. Furthermore, disrupting the expression of FOXM1 or the process of autophagosome-MVB transport impairs the loading of FOXM1-chDNAs to EVs. This discovery suggests that transcription factor FOXM1 contributes the constitution of evDNAs from nuclear chromatin, providing the first example to explain how chromatin DNA fragments are specified and loaded to EVs. It also provide a foundation to further explore the roles of evDNAs in biological processes such as the horizontal gene transfer.

Key words

Extracellular vesicle DNA; Transcription factor FOXM1; FOXM1-LC3 interaction; The process of autophagosome-MVB transport; Extracellular vesicles

32 **Introduction**

33 Extracellular vehicles (EVs) are membranous vesicles released by a variety of cells into the extracellular
34 microenvironment and contain DNAs, RNAs, and proteins acting as intercellular messengers for
35 exchanging variable materials among cells[1,2]. Because extracellular vesicle DNAs (evDNAs) carry the
36 portions of genetic materials from their parent cells under certain physiological or pathological
37 conditions, extensive studies have focused on the diagnostic value of evDNAs for multiple diseases,
38 while their biological functions are not explored as deeply as that of the RNAs or proteins of EVs[3,4]. The
39 evDNAs have been proposed to play a role in so called the horizontal gene transfer (HGT)[5], which allows
40 to exchange functional genes and DNA fragments among cells[6]. Increasing evidences support that EVs
41 contain functional genes or chromosome DNA fragments as evDNAs and transfer them to recipient cells[7].
42 For example, LINE-1 retrotransposon as an evDNA of EVs is horizontally transferred among human
43 cancer cells[8]. Another example is that Telomere DNA carried by the EVs from antigen-presenting cells
44 (APCs) is horizontally transferred to primarily naïve T cells and central memory T cells[9]. Therefore, it is
45 critical to understand how chromatin DNA fragments are specified and loaded to EVs, not only for
46 improving the application of evDNAs in diagnosis but also for clarifying their functions in biological
47 processes such as HGT.

48 Recently, chromatin DNA has been found to translocate to cytoplasm through the interaction
49 between laminB1 and LC3 in nucleus during autophagy[10], providing a clue to explore the origin of
50 evDNAs. LC3 is a key member of the Atg8 family proteins that are responsible for the cargo selection
51 of autophagy[11]. Besides existing in cytoplasm, LC3 is present in nucleus and interacts with the chromatin-
52 binding laminB1 (a nuclear lamina protein[12]). During autophagy, a part of regular LC3 (LC3-I) need be

53 conjugated with phosphatidyl ethanolamine (PE) to form LC3-PE (LC3-II), which is termed as the
54 lipidation of LC3 and allows the LC3 protein embedding in membranes and then loading cargos to
55 autophagosomes[13]. Although cytoplasmic autophagosomes fuse with endosomes or lysosomes to degrade
56 their components[14,15], accumulated evidences prove that a portion of endosomes fused with
57 autophagosomes can mature to form multivesicular bodies (MVBs, a special kind of late endosomes[16])
58 for the secretion of their cargos[1,17,18]. MVBs contain LC3-positive intraluminal vesicles (ILVs)[18], which
59 can be released to extracellular environment as EVs through the fusion of MVBs with cell membrane[2].
60 It's well known that LC3 specifies the loading of proteins and RNAs to EVs[18,19], confirming that variable
61 materials can be released by EVs through the process of an LC3-involved autophagosome-MVB
62 transport. However, because laminB1 possesses no sequence specificity for its DNA binding[20], it is hard
63 to figure out how certain chromatin DNA fragments are specified and loaded to EVs, if only basing on
64 the mechanism of laminB1-LC3-mediated chromatin DNA cytoplasmic translocation.

65 Here, we show a transcription factor-LC3-involved mechanism specifying certain chromatin genes
66 or DNA fragments to EVs during autophagy. FOXM1, a member of Forkhead Box transcription factor
67 family[21], participates in regulating cell proliferation[22], DNA damage repair[23], cell stemness[24], and
68 metastasis[25,26] through stimulating gene transcription in nucleus[27]. FOXM1 can specify its binding
69 regions on chromatin directly through its DNA-binding consensus sequence[28] or indirectly through
70 interacting with other transcription factors such as B-Myb, MuvB, and NFY[29]. In this study, we have
71 confirmed that FOXM1 interacts with LC3 in nucleus and mediates the loading of specific chromatin
72 DNA fragments (named FOXM1-chDNAs) to EVs during autophagy. The interaction between FOXM1
73 and LC3 is mediated by the LC3-interacting region motif of FOXM1 (317-320aa) and facilitated by the

lipidation of LC3, while the FOXM1-LC3 interaction does not disrupt the DNA binding ability of FOXM1. FOXM1-chDNAs, including *DUX4* gene and Telomere DNA, etc., have been identified by analyzing the sequencing data from FOXM1-specific ChIP-seq, LC3-specific ChIP-seq, and evDNA-seq. The loading of specific FOXM1-chDNAs to EVs has been confirmed by DNA-FISH experiments, tracing the translocation of selected chromatin loci with the TetO/TetR-GFP method, and PCR analysis of the DNA samples from MVBs and EVs. We have confirmed that the expression of FOXM1 or the process of LC3-involved autophagosome-MVB transport is essential for the loading of FOXM1-chDNAs to EVs. Together, this study has provided the first example to explain how chromatin DNA fragments are specified and loaded to EVs and a foundation to further explore the roles of evDNAs in biological processes such as HGT.

Results

The interaction between FOXM1 and LC3

LC3 mediated the loading of variable materials to EVs through the process of an LC3-involved autophagosome-MVB transport[18,19]. Interestingly, we identified LC3 as a potential partner interacting with transcription factor FOXM1, which directly or indirectly bound to the specific regions on chromatin, from our mass spectrometry analysis of the FOXM1 interactome (data not shown), implicating that FOXM1 might participate in specifying and loading chromatin DNA fragments to EVs. To test this hypothesis, we first confirmed the interaction between FOXM1 and LC3 in nucleus of lung cancer A549 cells. The immunostaining of endogenous FOXM1 and LC3 showed that the two proteins were co-localized in nucleus with the Pearson's Correlation Coefficient value around 0.66 ± 0.08 (**Fig. 1a**). The co-immunoprecipitation (co-IP) experiments revealed that FOXM1 interacted with LC3, especially with the lipidated LC3-II in nucleus (**Fig. 1b and Extended Data Fig. 1a, b**). A bimolecular fluorescence complementation (BiFC) assay[30] further confirmed that the FOXM1-LC3 interaction happened mainly in nucleus (**Fig. 1c**). The co-IP of exogenous Flag-FOXM1 with GFP-LC3 WT or G120A mutant, which disrupted the LC3 lipidation on its G120 residue[10], showed that the deficiency of the LC3 lipidation decreased the FOXM1-LC3 interaction (**Extended Data Fig. 1c, d**), implicating that LC3 embedding in nuclear membranes facilitated its interaction with FOXM1.

Next, we identified the regions of FOXM1 and LC3 to mediate the FOXM1-LC3 interaction. We screened FOXM1 protein and found that FOXM1 DNA-binding domain (FOXM1-DBD) was required for its LC3 binding (**Fig. 1d**) and FOXM1-DBD interacted with LC3 in GST-LC3-pulldown assays (**Fig. 1e**). Moreover, the overexpression of GFP-FOXM1-DBD abolished the endogenous FOXM1-LC3

105 interaction (**Extended Data Fig. 1e, f**). It was known that so-called LC3-interacting region (LIR) motif
106 existed in LC3' substrate proteins[31,32]. We screened the protein sequence of FOXM1-DBD and identified
107 four LIR motifs (263-266, 273-276, 307-310 and 317-320), which were evolutionarily conserved among
108 FOXM1s of human, mouse, rat, and macaque (**Extended Data Fig. 1g**). We generated four FOXM1-
109 DBD mutants (Y263A, F273A, F307A, and Y317A, corresponding to the four LIR motifs respectively),
110 among which only the Y317A mutation on FOXM1-DBD abolished its interaction with LC3 in GST-
111 LC3-pulldown assays (**Fig. 1f**), suggesting that the LIR motif (317-320) in FOXM1-DBD mediated the
112 binding of FOXM1 to LC3. On the other hand, because the residues R10, R11, and F52 of LC3 mediated
113 the binding of LC3 to its protein partners[10,33], we tested whether the LC3 aa1-28 region (containing R10
114 and R11) or the LC3 aa29-128 region (containing F52) could interact with FOXM1 in GST-pulldown
115 assays. We found that only the aa29-128 region (containing F52) of LC3 interacted with FOXM1 (**Fig.**
116 **1g**), implicating that the residues F52 of LC3 mediated the binding of LC3 to FOXM1. Thus, we
117 generated an LC3 aa29-128 truncated F52A mutant and found that this mutant could not bind to FOXM1
118 in GST-pulldown assays (**Fig. 1h**). Rosetta Dock[34] was performed with the known structures of FOXM1-
119 DBD[35] and LC3[36] to simulate the FOXM1-LC3 interaction and predicted the formation of hydrogen
120 bonds between the LIR motif (317-320) of FOXM1 and the residue F52 of LC3 (**Fig. 1i**), further
121 supporting the conclusion of the interaction between FOXM1 and LC3 in biochemical experiments.
122 To test whether the binding of LC3 to FOXM1-DBD affected the DNA-binding ability of FOXM1,
123 we performed the electrophoretic mobility shift assays (EMSAs) with recombinant FOXM1 proteins and
124 a FAM-labeled DNA probe containing putative FOXM1 binding sites. We observed that the DNA probe
125 formed FOXM1-DNA complexes with FOXM1 alone, and created a supershift of LC3-FOXM1-DNA

126 complexes by adding recombinant LC3 proteins in the reactions (**Fig. 1j**), suggesting that the FOXM1-
127 LC3 interaction did not impair the DNA-binding ability of FOXM1 and the LC3-FOXM1-DNA complex
128 could be formed in cells.

129 **FOXM1-chDNAs are loaded to extracellular vesicles during autophagy**

130 From the results of LC3 or FOXM1 immuno-staining and DNA DAPI-staining of A549 cells, we
131 observed that DNAs, FOXM1, and LC3 co-localized in cytoplasmic vesicles (**Fig. 2a and Extended**
132 **Data Fig. 2a**), whose numbers were increased by starvation-induced autophagy (from 3% in control cells
133 to 15% in starvation-treated cells) (**Fig. 2b**), suggesting that the formation of LC3-FOXM1-DNA vesicles
134 normally happened in cytoplasm and were enhanced during autophagy. Similar phenomena were also
135 observed from multiple human cancer cell lines, such as Hela and HEK293T cells, or the cells treated
136 with different autophagy-inducing conditions, such as No-amino acid, No-serum, or Rapamycin
137 treatment (20 μM) (data not shown). The BiFC assays with exogenous VN173-FOXM1 and VC155-LC3
138 further confirmed that FOXM1 and LC3 co-existed in cytoplasmic DNA-containing vesicles (**Fig. 2c**).
139 Interestingly, the expression of RFP-FOXM1 ΔDBD, in which FOXM1-DNA binding domain (DBD)
140 was deleted, could not appear in cytoplasmic DNA-containing vesicles (**Extended Data Fig. 2b**),
141 confirming that the FOXM1 DNA-binding ability was required for the formation of cytoplasmic LC3-
142 FOXM1-DNA vesicles during autophagy. Next, we collected EVs (including Large EVs (lEVs) and
143 Small EVs (sEVs)) from starved A549 cells by serial differential ultracentrifugation[37] (**Extended Data**
144 **Fig. 2c**). We showed that both FOXM1 and LC3 existed in the samples of EVs by Western blotting (**Fig.**
145 **2d**). Because researchers usually focused on sEVs when studying EVs[38,39] and only sEVs from our
146 samples possessed EV marker TSG101[40] (**Fig. 2d**), we just collected sEVs as EV samples in following

147 experiments and characterized their size range around 80-250 nm through nanoparticle tracking analysis
148 and transmission electron microscopy (**Extended Data Fig. 2d and e**). The DNA samples from EVs
149 (evDNAs) were purified and analyzed by the vertical agarose gel electrophoresis (**Fig. 2e**), which showed
150 the size range of evDNAs around 2 to 15 kb (majorly around 12 kb), confirming that DNA, FOXM1,
151 and LC3 co-existed in the samples of EVs.

152 To identify the chromatin DNA fragments specified by FOXM1 (FOXM1-chDNAs) that were
153 finally loaded to EVs, we first performed chromatin immunoprecipitation sequencing (ChIP-seq)
154 analysis for FOXM1 or LC3 separately with starved A549 cells and obtained 103 specific loci on
155 chromatin bound by both FOXM1 and LC3 (**Table S**) from the overlapping of FOXM1-ChIP fragments
156 (n=8, 838) (GSE216672) and LC3-ChIP fragments (n=7, 951) (GSE216672). Then we performed
157 evDNA-sequencing analysis with the EVs of starved A549 cells and obtained 15, 544 evDNAs
158 (GSE216672). After analyzing the overlapped sequences of FOXM1-LC3 ChIP loci and evDNAs, we
159 identified 25 chromatin loci as FOXM1-chDNAs (**Table**), which could be annotated as functional genes
160 (n=8, including *DUX4* gene), telomere (n=1), centromere (n=8), and nonsense regions (n=8). We chose
161 three FOXM1-chDNAs (FOXM1-chDNA1 from a telomere locus, FOXM1-chDNA2 from a nonsense
162 region, and FOXM1-chDNA3 from *DUX4* locus) as examples to perform ChIP-qPCR and confirmed the
163 binding of FOXM1 and LC3 on these FOXM1-chDNAs at chromatin but not on the control region such
164 as β-actin promoter (**Extended Data Fig. 2f, g**).

165 To verify that FOXM1-chDNAs were translocated to cytoplasm and finally loaded to EVs, we first
166 purified cytoplasmic DNA (cytoDNA) particularly[41] and found the levels of the three FOXM1-chDNAs
167 were elevated in cytoplasm of starved A549 cells (**Fig. 2f**). A DNA-FISH probe (10 Kb) specific for the

168 FOXM1-chDNA1-adjacent region was generated and DNA-FISH experiments showed that FOXM1-
169 chDNA1 appeared in cytoplasm post starvation (**Fig. 2g**), confirming that FOXM1-chDNAs were
170 translocated to cytoplasm during autophagy. Then, we purified evDNAs from the EVs of starved A549
171 cells and found the levels of the three FOXM1-chDNAs were elevated in the EVs (**Fig. 2h**), confirming
172 that FOXM1-chDNAs were finally loaded to EVs during autophagy. In addition, we also treated the EVs
173 of starved A549 cells with the Plasmid-Safe ATP-dependent DNase (PS), which only digested linear
174 DNA[42], and observed the decreased levels of the three FOXM1-chDNAs from the PS-treated samples
175 (**Extended Data Fig. 2h**), identifying that FOXM1-chDNAs existed as linear DNA on outside the lumen
176 of EVs. This result was consistent with the previous finding that evDNAs mainly localized on the outside
177 the lumen of EVs[43]. Then, we treated the EVs of starved A549 cells with formaldehyde to cross-link their
178 DNA and proteins and the lysates of EVs were immune-precipitated with anti-FOXM1 or anti-LC3
179 antibodies for evDNA purification. The levels of the three FOXM1-chDNAs in the FOXM1 or LC3
180 specific IP-evDNA samples were significantly elevated (**Fig. 2i**), further confirming that FOXM1-
181 chDNAs were bound by FOXM1 or LC3 on EVs. We also collected FOXM1-specific EVs or LC3-
182 specific EVs from GFP-FOXM1 or GFP-LC3-overexpressed A549 cells through the direct
183 immunoaffinity capture (DIC) approach[1] with GFP-Trap and observed the elevated levels of the three
184 FOXM1-chDNAs in the DIC samples (**Fig. 2j**), suggesting that both exogenous GFP-FOXM1 and GFP-
185 LC3 facilitated the loading of FOXM1-chDNAs to EVs. Together, these data suggested that FOXM1 and
186 LC3 mediated the loading of FOXM1-chDNAs to EVs during autophagy.

187 **The FOXM1-chDNAs knocked-in with the TetO array were loaded to EVs**

188 To confirm the translocation of FOXM1-chDNAs to EVs, we knocked in a TetO array (96x) at the loci

189 of selected FOXM1-chDNAs by CRISPR/cas9 in A549 cells (**Extended Fig. 3a**). DNAs containing the
190 TetO array then were visualized directly by exogenously expressed TetR-EGFP in cells[44]. Because
191 Telomere DNA was proved to load to EVs[9], we first edited the adjacent region of FOXM1-chDNA1 (a
192 Telomere locus) at chromosome 18 (**Extended Fig. 3b**) and observed the signal of TetO-Telomere in
193 nucleus followed by its elevated levels in cytoplasm post starvation (**Extended Fig. 3c, d**), confirming
194 the validity of the TetO/TetR-GFP method. Next, we edited the locus of FOXM1-chDNA3 (*DUX4* locus)
195 at chromosome 4 (**Extended Fig. 3b**) for following experiments. DUX4 was identified as a transcription
196 factor playing roles in embryonic development[45] and in promoting immune evasion of cancers[46]. The
197 signals of TetO array-containing DUX4 DNA (TetO-DUX4) could be visualized in nucleus of A549^{TetO-}
198 ^{DUX4} cells and its cytoplasmic signals were induced by starvation (**Fig. 3a**), which were further confirmed
199 by the qPCR results of the cytoDNA of TetO-DUX4 (**Fig. 3b**). The signal of TetO-DUX4 observed in
200 cytoplasm post starvation was co-localized with the immunofluorescent signal of LC3 (**Fig. 3c**),
201 confirming that FOXM1-chDNA3 (DUX4 locus) appeared in autophagosomes during autophagy.
202 Because autophagosomes could fuse with endosomes to mature to MVBs[16] that finally released their
203 cargos as EVs through fusing with cell membrane[2], we intended to test whether cytoplasmic TetO-DUX4
204 appeared in MVBs. We used the method of discontinuous sucrose gradient to prepare different fractions
205 to define MVB compartments[47] from postnuclear supernatants of A549$^{TetO-DUX4}$ cells. Based on the MVB
206 specific markers, such as Rab7[48], CD63[49], or TSG101[50], we first confirmed that FOXM1, same as LC3,
207 existed in the MVB fractions (**Fig. 3d**). The DNA samples were prepared from the harvested fractions
208 and the results of qPCR specific for TetO-DUX4 DNA showed its significant enrichment in the MVB
209 fractions (**Fig. 3e**). Furthermore, we observed that the signal of TetO-DUX4 in cytoplasm post starvation

210 was co-localized with the immunofluorescent signal of CD63 (**Fig. 3f**). We also isolated the samples of
211 MVBs by immunoprecipitating A549$^{TetO\text{-}DUX4}$ cell lysates with anti-CD63 antibodies[51] to prepare their
212 DNA, which showed the elevated levels of TetO-DUX4 DNA in these MVBs compared to the IgG-IP
213 controls (**Fig. 3g**), suggesting that this FOXM1-chDNA was transported to MVBs during autophagy.

214 We collected the EVs from A549 cells and A549$^{TetO\text{-}DUX4}$ cells to prepare DNA samples and the
215 results of PCR confirmed that TetO-DUX4 DNA appeared in EVs (**Fig. 3h**). The starvation in A549$^{TetO\text{-}}$
216 ^{DUX4} cells resulted in the elevated levels of TetO-DUX4 DNA in EVs (**Fig. 3i**). We also collected EVs
217 from A549$^{TetO\text{-}DUX4}$ cells through the DIC approach with anti-FOXM1 or anti-LC3 antibodies to prepare
218 DNA samples and observed the elevated levels of TetO-DUX4 DNA in the samples of FOXM1-specific
219 EVs or LC3-specific EVs (**Fig. 3j**), suggesting that FOXM1 and LC3 were involved in loading TetO-
220 DUX4 DNA to EVs. Moreover, after the EVs were treated with PS DNase, the decreased levels of TetO-
221 DUX4 DNA were observed but not for the mitochondrial DNA controls (**Fig. 3k**), implicating that TetO-
222 DUX4 DNA existed as linear DNA on the outer membrane of EVs. Together, we confirmed that this
223 FOXM1-chDNA was loaded to EVs during autophagy.

224 **The loading of FOXM1-chDNAs to EVs relied on FOXM1 and the autophagosome-MVB process**

225 We found that the PCR-amplified DNA samples from *DUX4* locus were able to pulled down FOXM1 or
226 lipidated LC3-II *in vitro* (**Fig. 4a**), proving the two proteins binding to this FOXM1-chDNA. To confirm
227 the roles of FOXM1 on the loading of FOXM1-chDNAs to EVs, we generated an A549$^{FOXM1\text{-}/\text{-}}$ cell line
228 by the CRISPR/cas9 technology targeting *FOXM1* gene in A549 cells (**Extended Data Fig. 4a**). In
229 A549$^{FOXM1\text{-}/\text{-}}$ cells, the levels of all the tested three FOXM1-chDNAs (FOXM1-chDNA1 from a telomere
230 locus, FOXM1-chDNA2 from a nonsense region, and FOXM1-chDNA3 from *DUX4* locus) were

231 decreased in cytoplasm compared to that of wild type control cells post starvation in the qPCR analysis
232 of purified cytoDNA samples (**Fig. 4b**). Consequently, the EVs from A549$^{FOXM1-/-}$ cells contained much
233 lower levels of the three FOXM1-chDNAs than that from control cells post starvation (**Fig. 4c**).
234 Furthermore, we knocked down the expression of FOXM1 in A549$^{TetO-DUX4}$ cells by FOXM1 siRNA
235 (**Extended Data Fig. 4b**) and observed that the cytoplasmic levels of TetO-DUX4 signals were decreased
236 in the cells post starvation (**Fig. 4d**). In addition, we constructed a linear DNA containing 72x FOXM1
237 binding sites (M1-binding DNA) that was bound by recombinant FOXM1 *in vitro* (**Extended Data Fig.**
238 **4c**) or FOXM1-DBD-GFP protein *in vivo* when transfected into cells (**Extended Data Fig. 4d**). We
239 transfected this M1-binding DNA or control DNA at the equal amount into cells and the qPCR analysis
240 of the isolated evDNA samples showed that the levels of M1-binding DNA in EVs were higher than that
241 of control DNA (**Fig. 4e**), suggesting that FOXM1 facilitated the FOXM1-recognized DNA fragments
242 transporting to EVs. We also transfected M1-binding DNA into A549$^{FOXM1-/-}$ cells and found that the
243 levels of M1-binding DNA in the EVs of A549$^{FOXM1-/-}$ cells were significantly lower than that of wild
244 type control cells (**Fig. 4f**). Together, the data suggested that the loading of FOXM1-chDNAs to EVs
245 relied on FOXM1 in cells.

246 To confirm the formation of autophagosomes contributing the loading of FOXM1-chDNAs to EVs,
247 we generated an A549$^{Atg5-/-}$ cell line by the CRISPR/cas9 technology targeting *Atg5* gene in A549 cells
248 (**Extended Data Fig. 4e**). It was well known that the Atg5 knockout resulted in the losing of LC3
249 lipidation and abolished the formation of autophagosomes[52,53]. In A549$^{Atg5-/-}$ cells, the cytoplasmic and
250 EVs' levels of the three FOXM1-chDNAs were lower than that of control cells post starvation (**Fig. 4g,**
251 **h**), correlated with the decreased levels of FOXM1 and LC3 in the EVs from A549$^{Atg5-/-}$ cells (**Extended**

252 **Data Fig. 4f**). In addition, we treated A549$^{TetO\text{-}DUX4}$ cells with 3-Methyladenine (3-MA), which prevented
253 the formation of autophagosomes[54], and observed that the cytoplasmic levels of TetO-DUX4 signals were
254 also decreased in the cells post starvation (**Fig. 4i**). To confirm the formation of MVBs contributing the
255 loading of FOXM1-chDNAs to EVs, we treated A549 cells with chloroquine (CQ), a lysosome inhibitor
256 that facilitated the formation of MVBs by inhibiting the fusion of MVBs and lysosomes[16,55]. We observed
257 that the levels of the three FOXM1-chDNAs were elevated in the EVs of the CQ-treated cells post
258 starvation (**Fig. 4j**). In addition, we treated A549 cells with a chemical compound GW4869, a neutral
259 sphingomyelinase inhibitor that prevented the fusion of MVBs with cell membrane and decreased the
260 secretion of EVs[56]. We collected the EVs from the equal numbers of A549 cells non-treated or treated
261 with GW4869 and found that the secretion of TSG101 via EVs was decreased by the GW4869 treatment,
262 confirming the abolished MVB-cell membrane fusion (**Extended Data Fig. 4g**). Consequently, the
263 secretion of FOXM1 or LC3 via EVs was also decreased by the GW4869 treatment (**Extended Data Fig.
264 4g**). Through the qPCR analysis of the prepared evDNA samples, we observed that the levels of the three
265 FOXM1-chDNAs in EVs, similar as that of mtDNA, were decreased by the GW4869 treatment,
266 suggesting that the secretion of FOXM1-chDNAs to EVs were majorly mediated by MVBs (**Fig. 4k**).
267 Together, the data suggested that the loading of FOXM1-chDNAs to EVs relied on the autophagosome-
268 MVB process.

269 **Discussion**

270 In this study, we have discovered that transcription factor FOXM1 mediates the loading of chromatin
271 DNA fragments to EVs. Specifically, certain FOXM1-bound chromatin DNA fragments (FOXM1-
272 chDNAs) form LC3-FOXM1-DNA vesicles with FOXM1 and LC3 in cytoplasm during autophagy. The

273 cytoplasmic LC3-FOXM1-DNAs are released to EVs through the process of an autophagosome-MVB
274 transport, providing an example of the transcription factor determining the sources of evDNA from
275 chromatin DNA (**Extended Data Fig. 5**). FOXM1 can theoretically specify its binding regions in
276 chromatin, providing a clue to determine the sources of evDNA from certain chromatin DNA loci. Based
277 on this understanding, the accuracy and specificity of disease diagnosis can be improved in the future by
278 focusing on specific sequences from patient evDNAs.

279 Although this study focuses on FOXM1, we anticipate that the FOXM1-LC3 interaction is not an
280 isolated event in nucleus. We have found that other Forkhead Box transcription factors such as FOXA2
281 and FOXP2 can interact with LC3 (data not shown), implicating that these two transcription factors may
282 also participate in determining the sources of evDNA from chromatin DNA. In addition, LC3 interacts
283 with multiple transcription factors that exist in EVs, based on the results of mass spectrometry
284 analysis[18,37], suggesting that these transcription factors may also play a similar role as FOXM1 for
285 specifying evDNA from chromatin DNA. Transcription factors are generally considered to bind to
286 specific DNA regions of chromosome and regulate specific gene expression in nucleus[57]. The findings
287 of this study expand the understanding of the functions of transcription factors and provide a new
288 perspective to explore their roles in regulating the composition of EVs' DNA components. Furthermore,
289 the further enrichment analysis of the specific sequences of patient evDNAs can predict certain
290 transcription factors that bind to the sequences, so as to establish the association between the transcription
291 factors and diseases to deduce the pathogenesis or disease progression.

292 The FOXM1-chDNAs identified in this study can be annotated as functional genes, telomere,
293 centromere, and nonsense regions, implicating their potential effects in the cells that receive these DNAs.

294 Interestingly, a recent study confirmed that Telomere DNAs carried by the EVs from antigen-presenting
295 cells can horizontally transfer to T cells and promote long-term immunological memory by rescuing T
296 cells from senescence[9]. We have observed the signals of TetO-DUX4 in recipient cells that are treated
297 with the A549$^{TetO\text{-}DUX4}$-derieved EVs and noticed the changes of phenotypes of recipient cells that are
298 transfected with the PCR-amplified DNA of *DUX4* locus (data not shown), providing another example
299 that the certain FOXM1-chDNAs of donor cells can perform specific biological functions in recipient
300 cells after the horizontal gene transfer (HGT) and may regulate the extracellular microenvironment of
301 the cells. Furthermore, because the EVs of local cells are able to enter the circulatory system, we
302 speculate that certain FOXM1-chDNAs may possess relevant roles in HGT to distant tissues. These
303 hypotheses are being investigated in our laboratory.

304 FOXM1 is generally considered as a transcription factor regulating gene expression in nucleus of
305 cells[27]. This study extends its function to loading certain chromatin DNA fragments to EVs. One key
306 question still remaining is how chromatin DNA breaks to specific fragments. So far, the appearance of
307 chromatin DNA in cytoplasm is mediated mainly by the micronuclei and cytoplasmic chromatin
308 fragment pathways[58], while both the mechanisms cannot explain the specific breakage of chromatin DNA.
309 Although nuclear LC3 interacts with LaminB1 to result in the cytoplasmic translocation of
310 transcriptionally inactive heterochromatin DNA[10], the mechanism of specific DNA fragments breaking
311 off chromosomes has not been explored. Recently, the complex of Rec114, Mei4 and Mer2 in cells has
312 been reported to control the precise DNA breakage[59], suggesting that the breakage of chromatin can be
313 precisely achieved. Future studies of FOXM1's interaction with the controlled DNA breakage machinery
314 will reveal how relevant chromatin DNA fragments are precisely produced.
315

316 **Methods**

317 **The complete Materials and Methods were described in Supplementary Materials.**

318 **ChIP sequencing, evDNA sequencing, Bioinformatics analysis, RT-qPCR.** For sequencing, ChIP and

319 evDNA samples were prepared as described previously[60]. The ChIP and evDNA were purified and used

320 for constructing sequencing libraries with a NEBNext Ultra DNA Library Prep Kit for Illumina (New

321 England Biolabs, Ipswich, MA, USA). The library quantifications were assessed on the Agilent

322 Bioanalyzer 2100 system. The library preparations were sequenced on an Illumina Hiseq platform and

323 50 bp single-end reads or 150 bp paired-end reads were generated.

324 For bioinformatics analysis, the following pipeline was used for analysis of all sequence data sets.

325 Firstly, fastp (version 0.20.0, parameter: '-q 15 -u 40 -n 6 -l 15 ')[61] was used to trim adaptors and low-

326 quality reads. Then, we evaluated the quality of NGS short reads by searching them on the FastQC

327 (version 0.11.8) program (http://www.bioinformatics.babraham.ac.uk/projects/fastqc). Thirdly, the

328 remaining reads were aligned to human genome hg38 by bwa men (version 0.7.17,parameter: '-t 20')[62],

329 since ChIP-Seq and evDNA-Seq interrupted fragments were usually small and the percentage of unique

330 sequences in the total number of sequences was the focus of attention. Finally, peak calling of the aligned

331 reads was made using macs3 (version 3.0.0a6, parameter: '-f BAM -g hs -p 0.1 -B')[63], and peaks were

332 annotated using the R/Bioconductor package ChIPseeker[64]. Browser views of peaks are shown using

333 Integrated Genomics Viewer (IGV; broadinstitute.org/igv)[65].

334 For qPCR, the following primers were used for qPCR analyses of chromatin loci. FOXM1-chDNA1

335 (chr18): forward, 5'-TGA TCA CCC AGG AGA CGG-3'; reverse, 5'-CTT GGG TGA TCA GTG GCG

336 AG-3'. FOXM1-chDNA2 (chr9): forward, 5'-CTG CAA AAT GGA CCA ATC AGC-3'; reverse, 5'-

337 AAG ATG GTG TGT CCG GAA TTT G-3'. FOXM1-chDNA3 (chr4): forward, 5'-TCA CAA GCC CCC

338 TGT AGG-3'; reverse, 5'-TCC AAC TCT TGC CTG GTC TC-3'.

339 **DNA Fluorescence *in situ* hybridization (FISH).** DNA-FISH probes were constructed by Exon
340 Biotechnology Inc (Guangzhou, China). The probes covered genomic regions (hg38) used in this study
341 was as follow: chr18: 103010-113570 (chr18_FOXM1-chDNA1_10 Kb). For fluorescence *in situ*
342 hybridization assay, DNA FISH was performed as described[66]. Briefly, coverslips containing fixed and
343 permeabilized cells were quenched by 3% H_2O_2, followed by dehydration in 70%, 85%, and 100%
344 ethanol for 1 min each. FISH probe (chr18_ FOXM1-chDNA1_10 Kb) was added onto a glass slide, and
345 lower the coverslips onto the slide slowly. Place the slides with samples to be hybridized in a heating
346 block at 85°C for 5min, and then 37°C for 20 hours. The slide was then removed, and the sample was
347 washed with Wash Buffer (1 X, preheated to 73°C) for 2 min. Added blocking buffer onto the hybridized
348 samples and incubated at 37°C for 30 min. Added primary antibody onto coverslip and incubated at 37°C
349 for 30 min. The sample was washed with Wash Buffer (1 X, preheated to 45°C) for 5 min. Added
350 secondary antibody onto coverslip and incubated at 37°C for 30 min. Wash coverslip in Wash Buffer (1x)
351 three times at 45°C for 5 min. Re-wash once with PBS. Preparation of TSA solution at TSA: 0.15%H2O2:
352 TSA amplification buffer = 1:5:500-1:10:1000. Add TSA solution to coverslip and incubate 5-15min at
353 RT. Wash coverslip in Wash Buffer (1 X) three times for 30 min. Mount coverslip with Anti-fade
354 Fluorescence Mounting Medium (with DAPI, Abcam, #ab104139).

355 **CRISPR/Cas9-mediated knock-in of a TetO array (96x) for visualization of FOXM1-chDNAs.** To
356 obtain a TetO-knockin cell line, we designed a pair of gRNAs using http://crispr.mit.edu/. The pair of
357 gRNAs (5'-CAC CTG GGT GAT CAG AGC AA-3' and 5'-TCT AGG CTT TGG CCT ACA GG-3')
358 bound to FOXM1-chDNA1 or gRNAs (5'-GCA GGC AGA GCG TAA GCA AA-3' and 5'-GGA CAC

359 ACG TTT AAT CGA GT-3') bound to FOXM1-chDNA3 was cloned into the pX335 vector (Addgene,
360 42335) before the gRNA scaffold. Furthermore, we designed two donor plasmids that contain the TetO
361 array (96x) flanked by 500-bp homology arms of the FOXM1-chDNAs in the pSP2-96-merTetO-EFS-
362 BLaR vector (Addgene, 118713). The primers (5'-CCC TTT CGT CTT CAA GAA TTC CAT CAC CTG
363 GGT GAT CAG TGT AGA-3', 5'-ACC CAT TCC TAG GGC GAA TTC GCT CTC TGA TCA CCC
364 AGG TGA T-3'; 5'-GCG CTGC TAG CTT AAG GTA CCA GCG TAG GCC AAA GCC TAG AC-3',
365 5'-CCC AGA TCT ATC GAT GGT ACC CTT GTC TAG GAT CTG CCT ACA GGG-3') were
366 synthesized and amplified homology arms of the FOXM1-chDNA1. The primers (5'- CCC TTT CGT
367 CTT CAA GAA TTC CCT GTA GGC AAG CCT ACA CAA GT-3', 5'-ACC CAT TCC TAG GGC GAA
368 TTC AGC GCT TAC GCT CTG CCT G-3'; 5'-GCG CTG CTA GCT TAA GGT ACC GAC CGA TTA
369 AAC GTG TGT CCT TT-3', 5'-CCC AGA TCT ATC GAT GGT ACC GTT TTT TCC TTT AAG ACT
370 TAT GTA ATG AAT T-3') were synthesized and amplified homology arms of the FOXM1-chDNA3. The
371 paired gRNAs and donor plasmids were co-transfected into A549 cells. Blasticidin (10 μg/ml) selection
372 was started 1 day after transfection. Three weeks after blasticidin selection, TetO-knockin cell clones
373 were transplanted into 24-well plates. Cells were collected from 24-well plates and extracted genomic
374 DNA (gDNA) for genotyping.

375 For FOXM1-chDNAs loci visualization, the TetO-knockin cells were transiently expressed with
376 TetR-EGFP. Cells were fixed in 4% paraformaldehyde and mounted with Mounting Medium with DAPI
377 (Abcam, ab104139). Images were captured by FV1200 laser scanning microscopes (Olympus, Japan).
378 For qPCR, the following primers were used for qPCR analyses of knock-in of FOXM1-chDNAs. TetO-
379 Telomere DNA (FOXM1-chDNA1 locus): forward, 5'-GAA GAC TAC AGC GTC GCC AG-3'; reverse,

380 5’-CGC GAC GAT ACA AGT CAG GT-3’. TetO-DUX4 DNA (FOXM1-chDNA3 locus): forward, 5’-
381 TCT GAA GAC TAC AGC GTC GC-3’; reverse, 5’-ACA CAT AAC CAG AGG GCA GC-3’.
382 **Extracellular vesicle isolation.** Cells seeded in 150 mm culture dishes at approximately 80% confluence
383 were incubated with serum-free DMEM for 1 day or 2 days. Cell viability was assessed using trypan blue
384 and only > 95% viability was used for EVs isolation. The cell-conditioned medium was collected by
385 sequential ultracentrifugation[1,18]. Briefly, the medium was first subjected to a centrifugation at 400 × g
386 for 10 min to remove cells. Next, the supernatant was centrifuged at 2,000 × g for 20 min to remove
387 debris and apoptotic bodies. Then, the supernatant was centrifuged at 15,000 × g for 40 min to obtain
388 large EVs. The resulting large EVs pellet was resuspended in a large volume of PBS buffer followed by
389 ultracentrifugation at 15,000 × g for 40 min to wash the sample. To remove any remaining any large EVs,
390 the media supernatant from the first 15,000 × g step was passed through a 0.22-μm pore PES filter
391 (Millipore, Bedford, MA, USA). This supernatant (pre-cleared medium) was next subjected to
392 ultracentrifugation at 120,000 × g for 4 h in a SW 28 Ti Swinging-Bucket Rotor (Beckman Coulter,
393 Fullerton, CA) to sediment small EVs. The crude small EVs pellet was resuspended in a large volume of
394 PBS followed by ultracentrifugation at 120,000 × g for 4 h to wash the sample. All following
395 centrifugation steps were performed at 4°C. Notably, for the comparison of EVs in different conditions,
396 the results must be corrected by total cell number or total protein concentration to eliminate differences
397 in cell seeding.

398 **Acknowledgements**

399 We thank Dr. Zhuoxian Rong of Central South University for help with construction of FOXM1 knockout
400 A549 cell line by CRISPR/Cas9 technology; thank Dr. Jianhui Jiang of Hunan University for help with
401 confocal microscopy. This work was supported by the National Natural Science Foundation of China
402 (grant number 81773169 to Y.T.), China Changsha Development and Reform Commission "Mass
403 entrepreneurship and innovation program" (2018-68) and "Innovation platform construction program"
404 (2018-216).

405 **Author contributions**

406 Y.Z. and Y.T. conceived this project. Y.Z., N.D., Y.L., X.Z., S.Y., H.L. and Y.W. performed all of
407 experiments. Y.Z., H.C., P.F., Y.P., L.Y. and T.Y. analyzed ChIP-seq and evDNA-seq. M.O. performed
408 molecular docking simulation. Y.C, L.Y. and X.H. provided administrative and material supports. Y.T.
409 supervised this study. Y.Z. and Y.T. composed the manuscript. All authors reviewed the manuscript and
410 discussed the work.

411 **Competing interests**

412 The authors declare no competing interests.

413 **Supplementary Material**

414 Supplementary methods, figures and tables.

415 **References**

416 1 Jeppesen, D. K. *et al.* Reassessment of Exosome Composition. *Cell* **177**, 428-445 e418 (2019).
417 2 van Niel, G., D'Angelo, G. & Raposo, G. Shedding light on the cell biology of extracellular
418 vesicles. *Nat Rev Mol Cell Biol* **19**, 213-228 (2018).
419 3 Sina, A. A. *et al.* Methylation dependent gold adsorption behaviour identifies cancer derived
420 extracellular vesicular DNA. *Nanoscale Horiz* **5**, 1317-1323 (2020).
421 4 Elzanowska, J., Semira, C. & Costa-Silva, B. DNA in extracellular vesicles: biological and
422 clinical aspects. *Mol Oncol* **15**, 1701-1714 (2020).
423 5 Douanne, N. *et al.* Leishmania parasites exchange drug-resistance genes through extracellular
424 vesicles. *Cell Rep* **40**, 111121 (2022).
425 6 Soucy, S. M., Huang, J. & Gogarten, J. P. Horizontal gene transfer: building the web of life. *Nat*
426 *Rev Genet* **16**, 472-482 (2015).
427 7 Cai, J., Wu, G., Jose, P. A. & Zeng, C. Functional transferred DNA within extracellular vesicles.
428 *Exp Cell Res* **349**, 179-183 (2016).
429 8 Kawamura, Y., Sanchez Calle, A., Yamamoto, Y., Sato, T. A. & Ochiya, T. Extracellular vesicles
430 mediate the horizontal transfer of an active LINE-1 retrotransposon. *J Extracell Vesicles* **8**,
431 1643214 (2019).
432 9 Lanna, A. *et al.* An intercellular transfer of telomeres rescues T cells from senescence and
433 promotes long-term immunological memory. *Nat Cell Biol* **24**, 1461-1474 (2022).
434 10 Dou, Z. *et al.* Autophagy mediates degradation of nuclear lamina. *Nature* **527**, 105-109 (2015).
435 11 Lee, Y. K. & Lee, J. A. Role of the mammalian ATG8/LC3 family in autophagy: differential and
436 compensatory roles in the spatiotemporal regulation of autophagy. *BMB Rep* **49**, 424-430 (2016).
437 12 Oldenburg, A. R. & Collas, P. Mapping Nuclear Lamin-Genome Interactions by Chromatin
438 Immunoprecipitation of Nuclear Lamins. *Methods Mol Biol* **1411**, 315-324 (2016).
439 13 Tanida, I., Ueno, T. & Kominami, E. LC3 and Autophagy. *Methods Mol Biol* **445**, 77-88 (2008).
440 14 Itakura, E., Kishi-Itakura, C. & Mizushima, N. The hairpin-type tail-anchored SNARE syntaxin
441 17 targets to autophagosomes for fusion with endosomes/lysosomes. *Cell* **151**, 1256-1269
442 (2012).
443 15 Diao, J. *et al.* ATG14 promotes membrane tethering and fusion of autophagosomes to
444 endolysosomes. *Nature* **520**, 563-566 (2015).
445 16 Fader, C. M. & Colombo, M. I. Autophagy and multivesicular bodies: two closely related
446 partners. *Cell Death Differ* **16**, 70-78 (2009).
447 17 Leidal, A. M. & Debnath, J. Emerging roles for the autophagy machinery in extracellular vesicle
448 biogenesis and secretion. *FASEB Bioadv* **3**, 377-386 (2021).
449 18 Leidal, A. M. *et al.* The LC3-conjugation machinery specifies the loading of RNA-binding
450 proteins into extracellular vesicles. *Nat Cell Biol* **22**, 187-199 (2020).
451 19 Leidal, A. M. & Debnath, J. LC3-dependent extracellular vesicle loading and secretion
452 (LDELS). *Autophagy* **16**, 1162-1163 (2020).
453 20 Gruenbaum, Y., Wilson, K. L., Harel, A., Goldberg, M. & Cohen, M. Review: nuclear lamins--
454 structural proteins with fundamental functions. *J Struct Biol* **129**, 313-323 (2000).
455 21 Costa, R. H., Kalinichenko, V. V., Holterman, A. X. & Wang, X. Transcription factors in liver

456 development, differentiation, and regeneration. *Hepatology* **38**, 1331-1347 (2003).
457 22 Fu, Z. *et al.* Plk1-dependent phosphorylation of FoxM1 regulates a transcriptional programme
458 required for mitotic progression. *Nat Cell Biol* **10**, 1076-1082 (2008).
459 23 Tan, Y., Raychaudhuri, P. & Costa, R. H. Chk2 mediates stabilization of the FoxM1 transcription
460 factor to stimulate expression of DNA repair genes. *Mol Cell Biol* **27**, 1007-1016 (2007).
461 24 Song, I. S. *et al.* FOXM1-Induced PRX3 Regulates Stemness and Survival of Colon Cancer
462 Cells via Maintenance of Mitochondrial Function. *Gastroenterology* **149**, 1006-1016 e1009
463 (2015).
464 25 Xie, Z. *et al.* Foxm1 transcription factor is required for maintenance of pluripotency of P19
465 embryonal carcinoma cells. *Nucleic Acids Res* **38**, 8027-8038 (2010).
466 26 Li, D. *et al.* The critical role of dysregulated FOXM1-PLAUR signaling in human colon cancer
467 progression and metastasis. *Clin Cancer Res* **19**, 62-72 (2013).
468 27 Sanders, D. A. *et al.* FOXM1 binds directly to non-consensus sequences in the human genome.
469 *Genome Biol* **16**, 130 (2015).
470 28 Marceau, A. H. *et al.* An order-to-disorder structural switch activates the FoxM1 transcription
471 factor. *Elife* **8**, e46131 (2019).
472 29 Liu, C., Barger, C. J. & Karpf, A. R. FOXM1: A Multifunctional Oncoprotein and Emerging
473 Therapeutic Target in Ovarian Cancer. *Cancers (Basel)* **13**2021).
474 30 Hu, C. D. & Kerppola, T. K. Simultaneous visualization of multiple protein interactions in living
475 cells using multicolor fluorescence complementation analysis. *Nat Biotechnol* **21**, 539-545
476 (2003).
477 31 Birgisdottir, A. B., Lamark, T. & Johansen, T. The LIR motif - crucial for selective autophagy.
478 *J Cell Sci* **126**, 3237-3247 (2013).
479 32 Johansen, T. & Lamark, T. Selective Autophagy: ATG8 Family Proteins, LIR Motifs and Cargo
480 Receptors. *J Mol Biol* **432**, 80-103 (2020).
481 33 Sentelle, R. D. *et al.* Ceramide targets autophagosomes to mitochondria and induces lethal
482 mitophagy. *Nat Chem Biol* **8**, 831-838 (2012).
483 34 Chaudhury, S. *et al.* Benchmarking and analysis of protein docking performance in Rosetta v3.2.
484 *PLoS One* **6**, e22477 (2011).
485 35 Littler, D. R. *et al.* Structure of the FoxM1 DNA-recognition domain bound to a promoter
486 sequence. *Nucleic Acids Res* **38**, 4527-4538 (2010).
487 36 Kuang, Y. *et al.* Structural basis for the phosphorylation of FUNDC1 LIR as a molecular switch
488 of mitophagy. *Autophagy* **12**, 2363-2373 (2016).
489 37 Hoshino, A. *et al.* Extracellular Vesicle and Particle Biomarkers Define Multiple Human
490 Cancers. *Cell* **182**, 1044-1061 e1018 (2020).
491 38 Moller, A. & Lobb, R. J. The evolving translational potential of small extracellular vesicles in
492 cancer. *Nat Rev Cancer* **20**, 697-709 (2020).
493 39 Gao, Y. *et al.* Small Extracellular Vesicles: A Novel Avenue for Cancer Management. *Front*
494 *Oncol* **11**, 638357 (2021).
495 40 Yoshioka, Y. *et al.* Comparative marker analysis of extracellular vesicles in different human
496 cancer types. *J Extracell Vesicles* **2**, eCollection 2013 (2013).
497 41 Abmayr, S. M., Yao, T., Parmely, T. & Workman, J. L. Preparation of nuclear and cytoplasmic

extracts from mammalian cells. *Curr Protoc Mol Biol* **Chapter 12**, Unit 12 11 (2006).

42 Wang, Y. *et al.* eccDNAs are apoptotic products with high innate immunostimulatory activity. *Nature* **599**, 308-314 (2021).

43 Liu, H. *et al.* Analysis of extracellular vesicle DNA at the single-vesicle level by nano-flow cytometry. *J Extracell Vesicles* **11**, e12206 (2022).

44 Tasan, I. *et al.* CRISPR/Cas9-mediated knock-in of an optimized TetO repeat for live cell imaging of endogenous loci. *Nucleic Acids Res* **46**, e100 (2018).

45 Hendrickson, P. G. *et al.* Conserved roles of mouse DUX and human DUX4 in activating cleavage-stage genes and MERVL/HERVL retrotransposons. *Nat Genet* **49**, 925-934 (2017).

46 Chew, G. L. *et al.* DUX4 Suppresses MHC Class I to Promote Cancer Immune Evasion and Resistance to Checkpoint Blockade. *Dev Cell* **50**, 658-671 e657 (2019).

47 de Araujo, M. E., Lamberti, G. & Huber, L. A. Homogenization of Mammalian Cells. *Cold Spring Harb Protoc* **2015**, 1009-1012 (2015).

48 Shearer, L. J. & Petersen, N. O. Distribution and Co-localization of endosome markers in cells. *Heliyon* **5**, e02375 (2019).

49 Piper, R. C. & Katzmann, D. J. Biogenesis and function of multivesicular bodies. *Annu Rev Cell Dev Biol* **23**, 519-547 (2007).

50 Nabhan, J. F., Hu, R., Oh, R. S., Cohen, S. N. & Lu, Q. Formation and release of arrestin domain-containing protein 1-mediated microvesicles (ARMMs) at plasma membrane by recruitment of TSG101 protein. *Proc Natl Acad Sci U S A* **109**, 4146-4151 (2012).

51 Ferreira, J. V. *et al.* LAMP2A regulates the loading of proteins into exosomes. *Sci Adv* **8**, eabm1140 (2022).

52 Klionsky, D. J. *et al.* Guidelines for the use and interpretation of assays for monitoring autophagy (4th edition)(1). *Autophagy* **17**, 1-382 (2021).

53 Otomo, C., Metlagel, Z., Takaesu, G. & Otomo, T. Structure of the human ATG12~ATG5 conjugate required for LC3 lipidation in autophagy. *Nat Struct Mol Biol* **20**, 59-66 (2013).

54 Seglen, P. O. & Gordon, P. B. 3-Methyladenine: specific inhibitor of autophagic/lysosomal protein degradation in isolated rat hepatocytes. *Proc Natl Acad Sci U S A* **79**, 1889-1892 (1982).

55 Mauthe, M. *et al.* Chloroquine inhibits autophagic flux by decreasing autophagosome-lysosome fusion. *Autophagy* **14**, 1435-1455 (2018).

56 Trajkovic, K. *et al.* Ceramide triggers budding of exosome vesicles into multivesicular endosomes. *Science* **319**, 1244-1247 (2008).

57 Todeschini, A. L., Georges, A. & Veitia, R. A. Transcription factors: specific DNA binding and specific gene regulation. *Trends Genet* **30**, 211-219 (2014).

58 Miller, K. N. *et al.* Cytoplasmic DNA: sources, sensing, and role in aging and disease. *Cell* **184**, 5506-5526 (2021).

59 Claeys Bouuaert, C. *et al.* DNA-driven condensation assembles the meiotic DNA break machinery. *Nature* **592**, 144-149 (2021).

60 Kharchenko, P. V., Tolstorukov, M. Y. & Park, P. J. Design and analysis of ChIP-seq experiments for DNA-binding proteins. *Nat Biotechnol* **26**, 1351-1359 (2008).

61 Chen, S., Zhou, Y., Chen, Y. & Gu, J. fastp: an ultra-fast all-in-one FASTQ preprocessor. *Bioinformatics* **34**, i884-i890 (2018).

62 Li, H. Aligning sequence reads, clone sequences and assembly contigs with BWA-MEM. *arXiv*, 1303.3997 (2013).

63 Zhang, Y. *et al.* Model-based analysis of ChIP-Seq (MACS). *Genome Biol* **9**, R137 (2008).

64 Yu, G., Wang, L. G. & He, Q. Y. ChIPseeker: an R/Bioconductor package for ChIP peak annotation, comparison and visualization. *Bioinformatics* **31**, 2382-2383 (2015).

65 Robinson, J. T. *et al.* Integrative genomics viewer. *Nat Biotechnol* **29**, 24-26 (2011).

66 Tsuchiya, K. D. Fluorescence in situ hybridization. *Clin Lab Med* **31**, 525-542, vii-viii (2011).

547 **Figure Legends**

548 **Figure 1. The interaction between FOXM1 and LC3. (a)** Representative FOXM1 and LC3 images in
549 A549 cells that were fixed by 4% paraformaldehyde and immunostained with anti-FOXM1 and anti-LC3
550 antibodies. Scale bar, 10 μm. The Pearson Correlation Coefficient (PCC) value of FOXM1 and LC3
551 colocalization was 0.66±0.08. **(b)** Co-immunoprecipitation of endogenous FOXM1 and LC3 in A549
552 cells. **(c)** The BiFC assays of FOXM1-LC3 interaction. HEK293T cells were transfected with the
553 indicated combination of split Venus constructs for 24 hrs. Scale bar, 10 μm. **(d)** HEK293T cells (5×10^6)
554 were transfected with Myc-tagged FOXM1 deletion mutant plasmids (5 μg). All cell lysates were pulled
555 down with bacterially purified GST-LC3 protein (30 μg) and subjected to immunoblotting as indicated.
556 **(e)** The GFP-fused FOXM1 truncations were expressed and pulled down with bacterially purified GST-
557 LC3 as described above. **(f)** The GFP-fused FOXM1-DBD point mutations were expressed and pulled
558 down with bacterially purified GST-LC3 as described above. **(g)** The Myc-tagged FOXM1 was pulled
559 down with bacterially purified GST-LC3 truncated mutants as described above. **(h)** The Myc-tagged
560 FOXM1 was expressed and pulled down with bacterially purified GST-LC3 truncated point mutants as
561 described above. **(i)** The molecular docking simulation for FOXM1-LC3 interaction by Rosetta Dock. **(j)**
562 EMSA showed FOXM1, LC3 and DNA formed LC3-FOXM1-DNA complex.

563 **Figure 2. FOXM1-chDNAs are loaded to extracellular vesicles during autophagy. (a)**
564 Representative LC3-FOXM1-DNA vesicles image in cytoplasm of starved A549 cells (6 hrs) that were
565 immunostained with anti-FOXM1 and anti-LC3 antibodies. The white arrows indicated LC3-FOXM1-
566 DNA vesicle. Scale bar, 10 μm. **(b)** Quantification of cytoplasmic LC3-FOXM1-DNA vesicle in non-

567 starved or starved A549 cells (6 hrs). (n = 4 independent experiments). **P<0.01; unpaired two-tailed.

568 **(c)** The BiFC assays showed that the exogenous VN173-FOXM1, VC155-LC3 and chromatin DNA

569 vesiculated in cytoplasm of starved A549 cells (6 hrs). Scale bar, 10 μm. **(d)** EVs were collected from

570 starved A549 cells (48 hrs) and subjected to immunoblotting for TSG101, FOXM1 and LC3. **(e)** evDNAs

571 were purified from EVs collected from starved A549 cells (48 hrs). The different concentrations of

572 evDNAs were analyzed by 1% vertical agarose gel electrophoresis. **(f)** The cytoplasmic DNA (cytoDNA)

573 was extracted from non-starved or starved A549 cells (24 hrs) for qPCR. The mitochondria DNA

574 (mtDNA, *ND-2* gene) was used as the internal loading control. The Bars, mean±s.e.m.; n=3; *P<0.05;

575 NS, non-significant; unpaired two-tailed. **(g)** Representative DNA-FISH images of FOXM1-chDNA1-

576 adjacent region (10 Kb probe) in starved A549 cells (6 hrs). The white arrows indicated FOXM1-

577 chDNA1. **(h)** The evDNA was extracted from non-starved or starved A549 cells (48 hrs) for qPCR. The

578 data were normalized by mtDNA. **(i)** The qPCR analyses of FOXM1-chDNAs in anti-FOXM1-IP

579 evDNA or anti-LC3-IP evDNA from EVs collected from starved A549 cells (48 hrs). **(j)** The qPCR

580 analyses of FOXM1-chDNAs in the DIC-purified GFP-FOXM1-specific EVs or DIC-purified GFP-

581 LC3-specific EVs collected from starved A549 stably expressing GFP-FOXM1 or GFP-LC3 cells (48

582 hrs). The Bars, mean±s.e.m.; n=3; *P<0.05, #P<0.05, **P<0.01; unpaired two-tailed.

583 **Figure 3. The FOXM1-chDNAs knocked-in with the TetO array were loaded to EVs. (a)**

584 Representative TetO-DUX4 images in starved A549$^{TetO\text{-}DUX4}$ cells (6 hrs) that were transiently expressed

585 TetR-EGFP. The white arrows indicated TetO-DUX4. Scale bar, 10 μm. **(b)** The A549$^{TetO\text{-}DUX4}$ cells were

586 treated with starvation and cytoplasmic DNA (cytoDNA) was extracted 24 hours later for qPCR. The

587 mtDNA was internal control. The Bars, mean±s.e.m.; n=3; **P<0.01; NS, non-significant; unpaired two-

588 tailed. **(c)** Immunostaining of the endogenous LC3 and TetO-DUX4 in starved A549$^{TetO\text{-}DUX4}$ cells (6 hrs)
589 that were exogenously expressed TetR-EGFP. The white arrows indicated TetO-DUX4 that was
590 translocated into cytoplasmic autophagosome. Scale bar, 10 μm. **(d)** MVB compartments were isolated
591 from starved A549$^{TetO\text{-}DUX4}$ cells (24 hrs) by discontinuous sucrose gradient and subjected to
592 immunoblotting. **(e)** The qPCR analyses of TetO-DUX4 in MVB fractions collected from starved
593 A549$^{TetO\text{-}DUX4}$ cells (24 hrs) by discontinuous sucrose gradient. The Bars, mean±s.e.m.; n=3; $^{**}P<0.01$;
594 NS, non-significant; unpaired two-tailed. **(f)** Immunostaining of the endogenous CD63 and TetO-DUX4
595 in starved-A549$^{TetO\text{-}DUX4}$ cells (6 hrs). The white arrows indicated TetO-DUX4 that was translocated into
596 cytoplasmic MVB. Scale bar, 10 μm. **(g)** The qPCR analyses of TetO-DUX4 in MVBs collected from
597 starved-A549$^{TetO\text{-}DUX4}$ cells (24 hrs) by CD63-immunoprecipitation. The Bars, mean±s.e.m.; n=3;
598 $^{**}P<0.01$; NS, non-significant; unpaired two-tailed. **(h)** PCR was used to amplify the TetO-DUX4,
599 DUX4, and mitochondria DNAs in the evDNAs collected from starved A549^{WT} or A549$^{TetO\text{-}DUX4}$ cells (48
600 hrs). **(i)** The qPCR analyses of TetO-DUX4 in the EVs collected from starved-A549$^{TetO\text{-}DUX4}$ cells (48
601 hrs). **(j)** The qPCR analyses of TetO-DUX4 in the DIC-purified FOXM1-specific EVs or LC3-specific
602 EVs collected from starved-A549$^{TetO\text{-}DUX4}$ cells (48 hrs). **(k)** The qPCR analyses of TetO-DUX4 in the
603 Plasmid-Safe ATP-dependent DNase (PS)-digested EVs collected from starved-A549$^{TetO\text{-}DUX4}$ cells. The
604 Bars, mean±s.e.m.; n=3; $^{*}P<0.05$; $^{\#}P<0.05$; $^{**}P<0.01$; $^{\#\#}P<0.01$; unpaired two-tailed.

605 **Figure 4. The loading of FOXM1-chDNAs to EVs relied on FOXM1 and the autophagosome-MVB**
606 **process. (a)** A549 cell lysates were incubated with biotinylated DUX4 DNA (500 ng). The bound
607 proteins were immunoprecipitated with streptavidin microbeads and blotted by anti-FOXM1 or LC3
608 antibodies. **(b, c)** The qPCR analyses of three FOXM1-chDNAs in the cytoplasm or EVs collected from

609 starved A549 or A549$^{FOXM1-/-}$ cells. The data were normalized by mtDNA. The Bars, mean±s.e.m.; n=3;

610 **P<0.01; unpaired two-tailed. **(d)** A549$^{TetO-DUX4}$ cells were transfected with 50 nM *FOXM1* siRNA and

611 1 μg TetR-EGFP plasmid. After the transfection (48 hrs), cells were starved (6 hrs) and imaged for the

612 signal of TetO-DUX4 (left). The white arrows indicated TetO-DUX4. Scale bar, 10 μm. The TetO-DUX4

613 signal in cytoplasm was quantitated (right). n = 3 independent experiments; *P<0.05; unpaired two-tailed.

614 **(e)** HEK293T cells were transfected with linear M1-binding or control DNA at the equal amount. After

615 the transfection (24 hrs), all cells were starved (48 hrs) for collecting EVs**.** The qPCR analyses were

616 performed for the mtDNA and transfected DNA in evDNAs purified from the EVs. **(f)** A549 and

617 A549$^{FOXM1-/-}$ cells were transfected with linear M1-binding DNA at the equal amount. After the

618 transfection (24 hrs), all cells were starved (48 hrs) for collecting EVs**.** The qPCR analyses were

619 performed for the mtDNA and transfected DNA in evDNAs purified from the EVs. The Bars,

620 mean±s.e.m.; n=3; *P < 0.05; **P<0.01; NS, non-significant; unpaired two-tailed. **(g, h)** The qPCR

621 analyses of three FOXM1-chDNAs in the cytoplasm or EVs collected from starved A549 or A549$^{Atg5-/-}$

622 cells. The data were normalized by mtDNA. The Bars, mean±s.e.m.; n=3; **P<0.01; unpaired two-tailed.

623 **(i)** A549$^{TetO-DUX4}$ cells were transfected with TetR-EGFP plasmid (1 μg). After the transfection (24 hrs),

624 cells were treated with 3-MA (5 mM) and starved (6 hrs). Cells were immunostained with anti-LC3

625 antibodies and imaged for TetO-DUX4. The white arrows indicated the signal of TetO-DUX4. Scale bar,

626 10 μm. The TetO-DUX4 signal in cytoplasm was compared (right). n = 3 independent experiments;

627 *P<0.05; unpaired two-tailed. **(j)** EVs were collected from A549 cells that were treated with CQ (20 μM)

628 and starvation (24 hrs). The qPCR analyses were performed for the three FOXM1-chDNAs in evDNAs

629 purified form the EVs. **(k)** EVs were collected from A549 cells that were treated with GW4869 (20 μM)

630 and starvation (24 hrs). The qPCR analyses were performed for the three FOXM1-chDNAs in evDNAs

631 purified form the EVs.

632 **Figure 1**

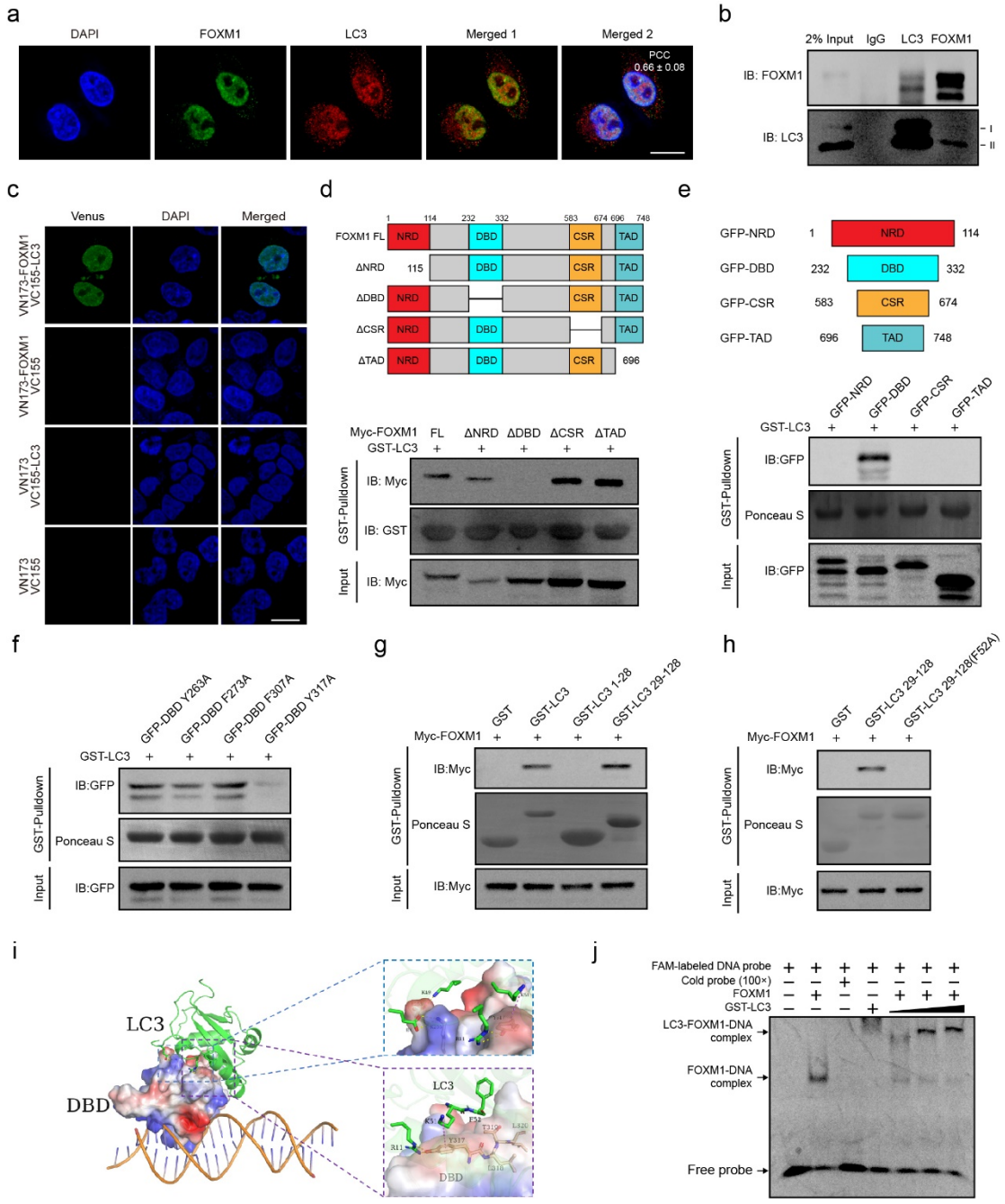

633

634

Figure 2

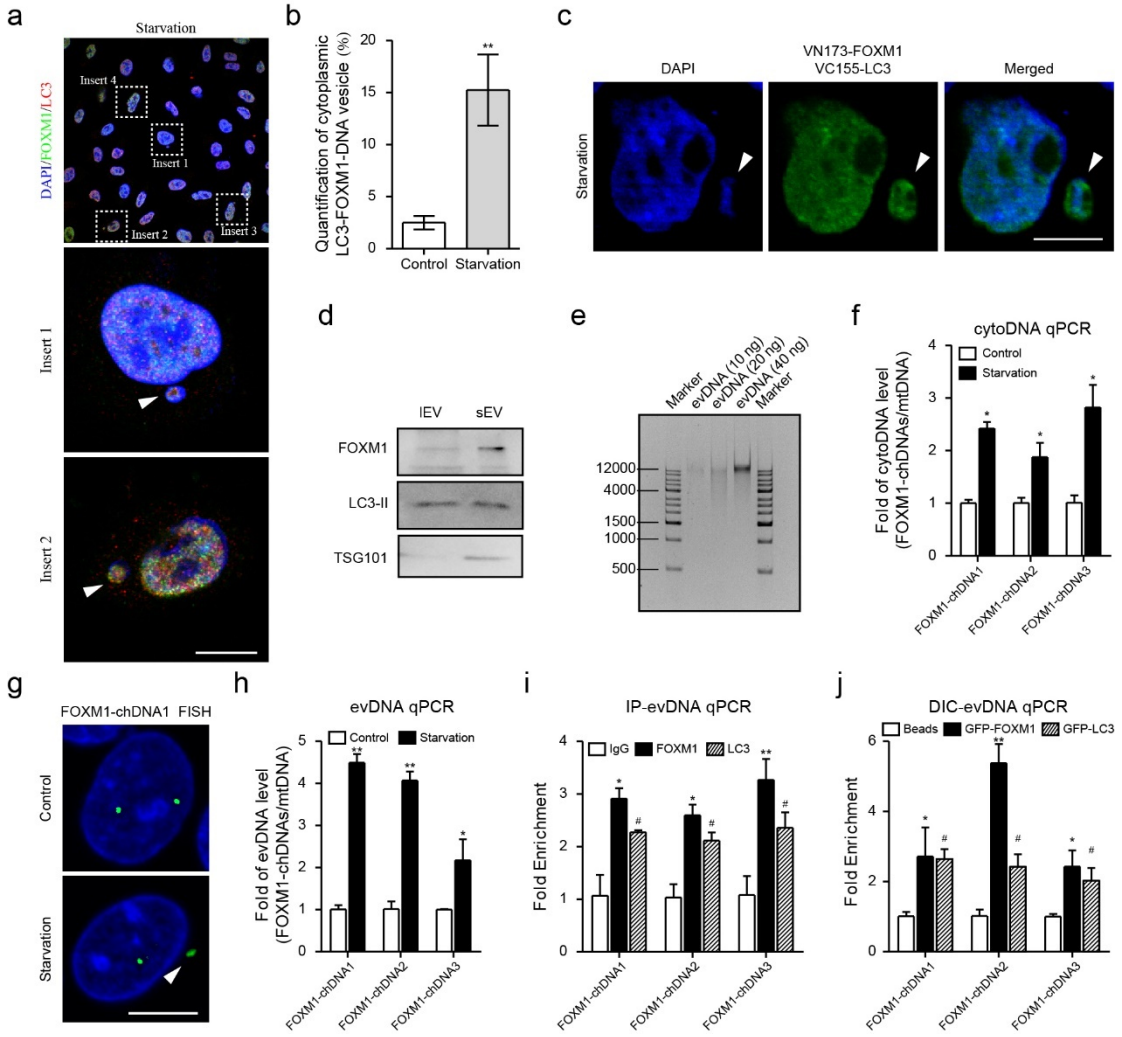
a
Starvation
DAPI/FOXM1/LC3
Insert 4
Insert 1
Insert 2
Insert 3
Insert 1
Insert 2
b
Quantification of cytoplasmic LC3-FOXM1-DNA vesicle (%)
Control
Starvation
c
DAPI
VN173-FOXM1
VC155-LC3
Merged
Starvation
d
lEV
sEV
FOXM1
LC3-II
TSG101
e
Marker
evDNA (10 ng)
evDNA (20 ng)
evDNA (40 ng)
Marker
12000
4000
1500
1000
500
f
cytoDNA qPCR
Control
Starvation
Fold of cytoDNA level (FOXM1-chDNAs/mtDNA)
FOXM1-chDNA1
FOXM1-chDNA2
FOXM1-chDNA3
g
FOXM1-chDNA1 FISH
Control
Starvation
h
evDNA qPCR
Control
Starvation
Fold of evDNA level (FOXM1-chDNAs/mtDNA)
FOXM1-chDNA1
FOXM1-chDNA2
FOXM1-chDNA3
i
IP-evDNA qPCR
IgG
FOXM1
LC3
Fold Enrichment
FOXM1-chDNA1
FOXM1-chDNA2
FOXM1-chDNA3
j
DIC-evDNA qPCR
Beads
GFP-FOXM1
GFP-LC3
Fold Enrichment
FOXM1-chDNA1
FOXM1-chDNA2
FOXM1-chDNA3

638 **Figure 3**

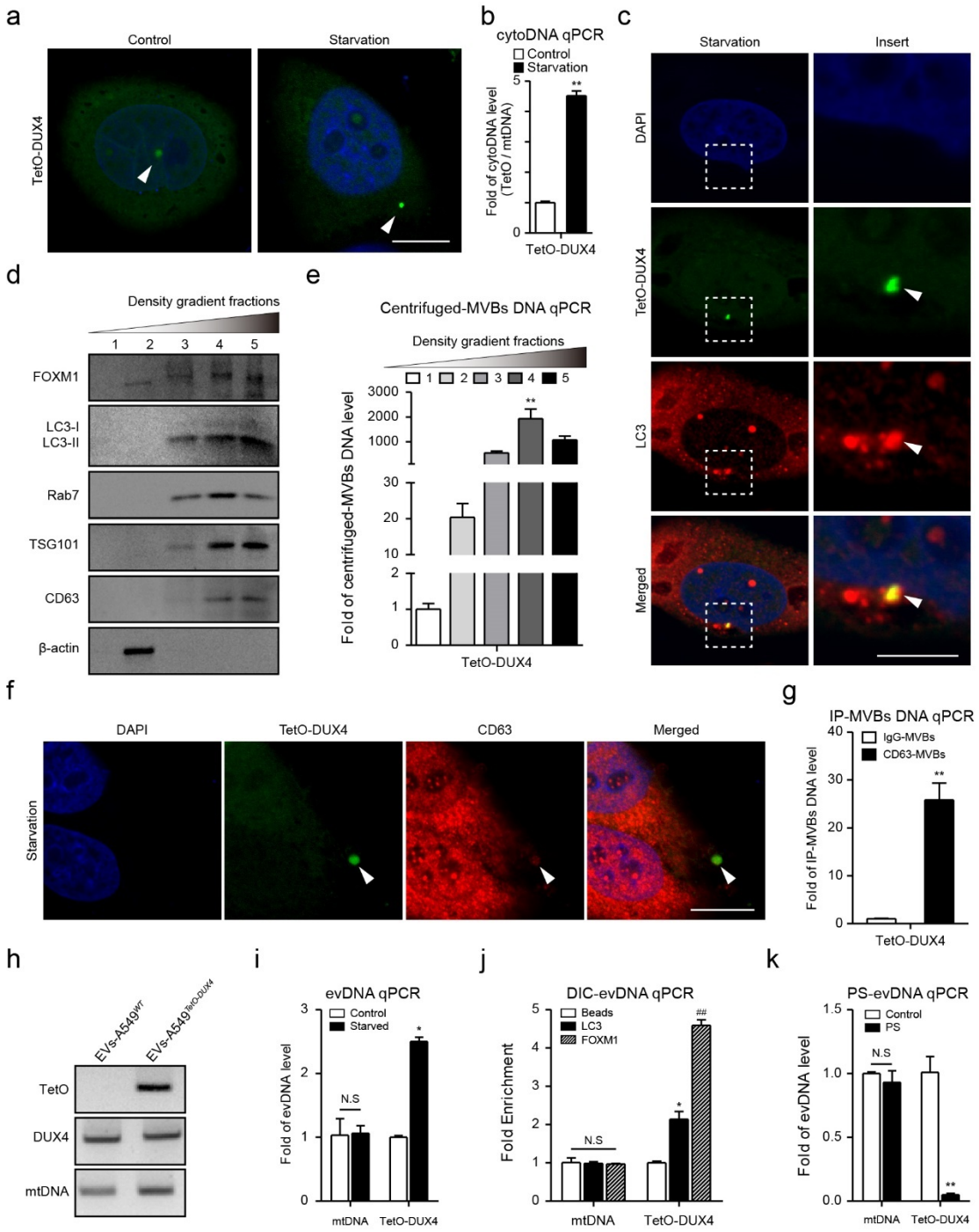

639

640

641 **Figure 4**

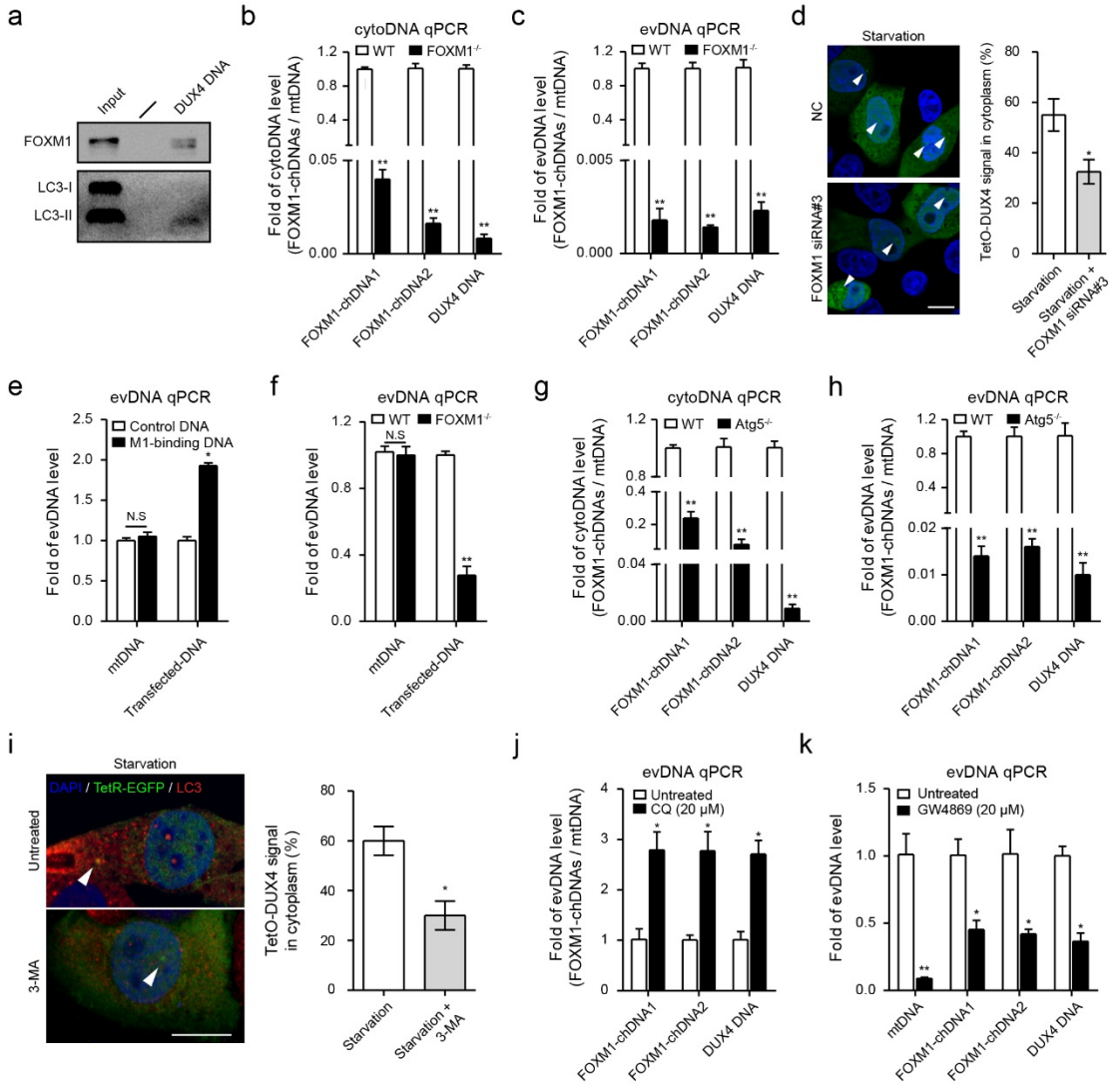

642
643

644 **Table. FOXM1-chDNAs.**

Names	Sequence signatures	Chr	geneID
FOXM1-chDNA1	Telomere	18	ENSG00000263006
FOXM1-chDNA2	Nonsense region	9	ENSG00000228522
FOXM1-chDNA3	Coding region (*DUX4*)	4	ENSG00000260596
FOXM1-chDNA4	Coding region (*PGK1*)	X	ENSG00000102144
FOXM1-chDNA5	Coding region (*ITFG2*)	12	ENSG00000111203
FOXM1-chDNA6	Coding region (*FOXM1*)	12	ENSG00000111206
FOXM1-chDNA7	Coding region (*FOXM1*)	12	ENSG00000111206
FOXM1-chDNA8	Coding region (*TBC1D5*)	3	ENSG00000131374
FOXM1-chDNA9	Coding region (*XR_946063.2*)	10	ENSG00000166317
FOXM1-chDNA10	Coding region (*XR_943570.1*)	14	ENSG00000258314
FOXM1-chDNA11	Centromere	5	ENSG00000170571
FOXM1-chDNA12	Centromere	1	ENSG00000224857
FOXM1-chDNA13	Centromere	20	ENSG00000227195
FOXM1-chDNA14	Centromere	3	ENSG00000251727
FOXM1-chDNA15	Nonsense region	16	ENSG00000261239
FOXM1-chDNA16	Nonsense region	16	ENSG00000261239
FOXM1-chDNA17	Nonsense region	16	ENSG00000261239
FOXM1-chDNA18	Nonsense region	16	ENSG00000261239
FOXM1-chDNA19	Nonsense region	16	ENSG00000261239
FOXM1-chDNA20	Centromere	17	ENSG00000263433
FOXM1-chDNA21	Centromere	17	ENSG00000263433
FOXM1-chDNA22	Centromere	17	ENSG00000263433
FOXM1-chDNA23	Centromere	17	ENSG00000264970
FOXM1-chDNA24	Nonsense region	1	ENSG00000276118
FOXM1-chDNA25	Nonsense region	5	ENSG00000284042

645